



# Edge smoothness enhancement in DMD scanning lithography system based on a wobulation technique

RONGHUAN CHEN,<sup>1</sup> HUA LIU,<sup>1,\*</sup> HAOLIN ZHANG,<sup>2,3</sup> WENJUAN ZHANG,<sup>1</sup> JIA XU,<sup>3</sup> WENBIN XU,<sup>3</sup> AND JINHUAN LI<sup>1</sup>

<sup>1</sup>Center for Advanced Optoelectronic Functional Materials Research, and Key Laboratory for UV-Emitting Materials and Technology of Ministry of Education, Northeast Normal University, 5268 Renmin Street, Changchun 130024, China

<sup>2</sup>Departamento de Física, Universitat Autònoma de Barcelona, Bellaterra 08193, Spain

<sup>3</sup>Changchun Institute of Optics, Fine Mechanics and Physics, Chinese Academy of Sciences, Changchun 130033, China

\*liuhua\_rain@aliyun.com

**Abstract:** The resolution of digital micro-mirror device (DMD) scanning lithography is limited in the transverse direction (the scanning direction is vertical) as a result of the compacted size of the DMD micro-mirror and the low magnification of the projection lens. Above-stated restrictions lead to an unsatisfactory saw-tooth edge (size ~one DMD pixel) after the lithography process within all directions except for the scanning orientation. In order to smooth the edge, an optimized sub-pattern construction method, described as the combination of wobulation techniques and the continuous scanning lithography process, is proposed. Afterward, lithography experiments were implemented by introducing the wobulation techniques within the DMD scanning lithography system. The experimental results show that the saw-tooth edge is reduced to nearly 0.5 pixel size after 1/2 pixel dislocation superposition exposure, and is even scaled down to less than 0.1 pixel after 1/4 pixel dislocation superposition exposure. At this point, the edge of the lithography pattern is appropriately smoothed. The effectiveness of the above-mentioned method that improves the edge smoothness of the lithography pattern is demonstrated.

© 2017 Optical Society of America

**OCIS codes:** (220.3740) Lithography; (220.4000) Microstructure fabrication.

## References and links

1. K. Wu, T. Rindzevicius, M. S. Schmidt, K. B. Mogensen, S. Xiao, and A. Boisen, "Plasmon resonances of Ag capped Si nanopillars fabricated using mask-less lithography," *Opt. Express* **23**(10), 12965–12978 (2015).
2. H. Wu, W. Hu, H. C. Hu, X. W. Lin, G. Zhu, J. W. Choi, V. Chigrinov, and Y. Q. Lu, "Arbitrary photo-patterning in liquid crystal alignments using DMD based lithography system," *Opt. Express* **20**(15), 16684–16689 (2012).
3. S. E. Chung, W. Park, H. Park, K. Yu, N. Park, and S. Kwon, "Optofluidic mask-less lithography system for real-time synthesis of photopolymerized microstructures in microfluidic channels," *Appl. Phys. Lett.* **91**(4), 041106 (2007).
4. S. H. Song, K. Kim, S. E. Choi, S. Han, H. S. Lee, S. Kwon, and W. Park, "Fine-tuned grayscale optofluidic maskless lithography for three-dimensional freeform shape microstructure fabrication," *Opt. Lett.* **39**(17), 5162–5165 (2014).
5. D. Dendukuri, D. C. Pregibon, J. Collins, T. A. Hatton, and P. S. Doyle, "Continuous-flow lithography for high-throughput microparticle synthesis," *Nat. Mater.* **5**(5), 365–369 (2006).
6. P. Panda, S. Ali, E. Lo, B. G. Chung, T. A. Hatton, A. Khademhosseini, and P. S. Doyle, "Stop-flow lithography to generate cell-laden microgel particles," *Lab Chip* **8**(7), 1056–1061 (2008).
7. K. W. Bong, J. J. Kim, H. Cho, E. Lim, P. S. Doyle, and D. Irimia, "Synthesis of Cell-Adhesive Anisotropic Multifunctional Particles by Stop Flow Lithography and Streptavidin-Biotin Interactions," *Langmuir* **31**(48), 13165–13171 (2015).
8. J. Lee, P. W. Bisso, R. L. Srinivas, J. J. Kim, A. J. Swiston, and P. S. Doyle, "Universal process-inert encoding architecture for polymer microparticles," *Nat. Mater.* **13**(5), 524–529 (2014).
9. S. E. Chung, W. Park, S. Shin, S. A. Lee, and S. Kwon, "Guided and fluidic self-assembly of microstructures using railed microfluidic channels," *Nat. Mater.* **7**(7), 581–587 (2008).

10. D. Dendukuri, S. S. Gu, D. C. Pregibon, T. A. Hatton, and P. S. Doyle, "Stop-flow lithography in a microfluidic device," *Lab Chip* **7**(7), 818–828 (2007).
11. K. Totsu, K. Fujishiro, S. Tanaka, and M. Esashi, "Fabrication of three-dimensional microstructure using maskless gray-scale lithography," *Sens. Actuators A Phys.* **130–131**(2), 387–392 (2006).
12. X. Y. Ding, Y. X. Ren, L. Gong, Z. X. Fang, and R. D. Lu, "Microscopic lithography with pixelate diffraction of a digital micro-mirror device for micro-lens fabrication," *Appl. Opt.* **53**(24), 5307–5311 (2014).
13. S. A. Lee, S. E. Chung, W. Park, S. H. Lee, and S. Kwon, "Three-dimensional fabrication of heterogeneous microstructures using soft membrane deformation and optofluidic maskless lithography," *Lab Chip* **9**(12), 1670–1675 (2009).
14. Y. M. Ha, I. B. Park, H. C. Kim, and S. H. Lee, "Three-dimensional microstructure using partitioned cross-sections in projection microstereo lithography," *Int. J. Precis. Eng. Manuf.* **11**(2), 335–340 (2010).
15. N. Hakimi, S. S. H. Tsai, C. H. Cheng, and D. K. Hwang, "One-Step Two-Dimensional Microfluidics-Based Synthesis of Three-Dimensional Particles," *Adv. Mater.* **26**(9), 1393–1398 (2014).
16. K. Kim, S. Han, J. Yoon, S. Kwon, H. K. Park, and W. Park, "Lithographic resolution enhancement of a maskless lithography system based on a wobulation technique for flow lithography," *Appl. Phys. Lett.* **109**(23), 234101 (2016).
17. W. Allen and R. Ulichney, 47.4: Invited paper, "Wobulation: Doubling the addressed resolution of projection displays," in *SID Symposium Digest of Technical Papers*, Blackwell Publishing Ltd. (2005), pp. 1514–1517.
18. J. M. Younse, "Mirrors on a chip," *Spectrum* (IEEE, 1993), pp. 27–31.
19. B. Sampsel, "Digital micro-mirror device and its application to projection displays," *J. Vac. Sci. Technol. B* **12**(6), 3242–3246 (1994).

## 1. Introduction

The interests of using DMD digital lithography as a new mask-less lithography have been widely discussed nowadays. For instance, it not only improves the production efficiency and reduces the production cost, but also provides a broad prospect in the field of lithography compare to single point laser direct writing technique. With the improvement in DMD drive technology, a high frame frequency of more than 20k-Hz is achieved. Note that such high frequency outfits the feasibility of the continuous rolling scanning exposure mode [1–4]. Under this scenario, DMD digital lithography is widely used in various fields such as printed circuit board, chip fabrication, bioassays, drug-delivery, cell carriers, tissue-engineering and so on [5–10]. What is more, the improvements in scanning mask-less lithography provide the feasibility to achieve large area, high efficiency fabrication. For instance, numbers of microstructures represented as microlens array, hydrogel encapsulation structure, free-floating polymer wire and et al. are achieved by DMD scanning lithography. We want to emphasize that not only a three-dimensional moving stage [11, 12], but also an optofluidic channel can provide the scanning process [13]. In our paper, we mainly focus on the smoothness of the microstructure fabricated by the DMD scanning lithography. In this case, even though the edge smoothness of the lithography pattern can be improved by the micro-mirror light spot superposition in the scanning direction during the writing, it is relatively poor in other directions, leads to a deficient saw-tooth structure at the line edge.

The conventional approach to improve the smoothness of the lithography pattern edge is to reduce the magnification of the projection lens [14]. Afterward, by improving the optical resolution, the saw-tooth edge pattern can be enhanced. Although this method can improve the smoothness of the lithography pattern edge to a certain extent, the single exposure area is also greatly reduced, leads to the reduction in production efficiency. What is more, a high accuracy within the adjustment of the imaging system and an accurate focusing process during the lithography experiment are required. Gray-scale exposure imaging technology [15] demonstrates its ability to control a tiny fraction of the line width in a pixel to improve the smoothness of the lithography pattern edge as well. However, each frame data cannot be simply replaced by rolling, but requires special transformation, which increases the difficulty in data processing, hardware storage and computing capacity.

A method to improve the resolution of the lithography pattern in the DMD lithography using a wobulation technique [16, 17] is presented recently. By introducing wobulation technique, multiple sub-frames suited to static exposure are generated from the image data in the first place, and are projected on slightly different positions on the screen afterward. We

noticed that, by implementing the wobulation technique, the edge smoothness of the lithography pattern is improved to a certain extent. However, the exposure process proposed by the motorized stage vibration in [16], is in fact a static exposure, which cannot satisfy a large area exposure (i.e., PCB board, linear scale fabrication). Moreover, the static exposure proposed by Kim et al. can only optimize the exposure energy discontinuity among the adjacent micro-mirrors (leads to a bumpy surface) by multiple exposures within their corresponding frames, which decreases the efficiency.

In this paper, we apply the wobulation technique to the DMD continuous scanning lithography to improve the smoothness of the lithography pattern edge. A basic principle demonstrated as constructing sub-patterns matching with subsequent scanning exposures (provided by a moving platform) is introduced first. These sub-patterns are programmed into the DMD in an experimental predetermined order, which create a high frame data by scrolling update. These high frame data and the moving platform cooperate with each other to perform a continuous scanning exposure so as to complete the scanning exposure superposition of the sub-patterns on the photoresist substrate. Under this scenario, our method (i.e., continuous single-direction scanning exposure) can promise a large area exposure, as well as enhance the edge smoothness. For the sake of the introduction of the continuous exposure, a more efficient sub-pattern choosing method which mainly focuses on the pattern margin is proposed. Hence, flexible sub-patterns can be generated. Last but not least, by providing the single displacement direction exposure, a mechanic offset error is avoided within the moving platform. As a result, the saw-tooth of the lithography pattern edge is reduced from the original 1 pixel size to less than 0.1 pixel size. The edges of the lithography patterns show a good smoothness. The edge smoothness of the lithography pattern indicates the correctness and the effectiveness of DMD scanning lithography based on the wobulation technique.

## 2. DMD based sub-patterns matching wobulation lithography technique

Figure 1 shows the DMD lithography scheme, including the light source, the spatial light modulator (DMD), the projection lens, the precision moving platform and the controlling system. The laser beam emitted from the light source is collimated and uniformed by the optical elements, and then is reflected to the DMD. Afterward, the image generated by the DMD is projected on the substrate placed on the precision moving platform by the projection lens. Finally, the generated patterns amplified by the projection lens, is written on the substrate. In our experiment, the lithography system uses a 0.95 inches DMD chip with a  $1920 \times 1080$  array, and each micro-mirror is of  $10.68 \mu\text{m} \times 10.68 \mu\text{m}$ . A laser with a wavelength of 405 nm is chosen as the light source. A projection lens with a magnification of one is used as the projector. The SU8 photoresist coated on the substrate is used as the photosensitive material.

By comparing to the static exposure lithography system, our proposed lithography system uses a two dimensional moving stage which can provide a larger exposure area as well as a higher precision with a high displacement speed. What is more, the continuous scanning exposure in our implementation is achieved by choosing a high frequency frame, large efficient area DMD which provides a high speed data scroll.

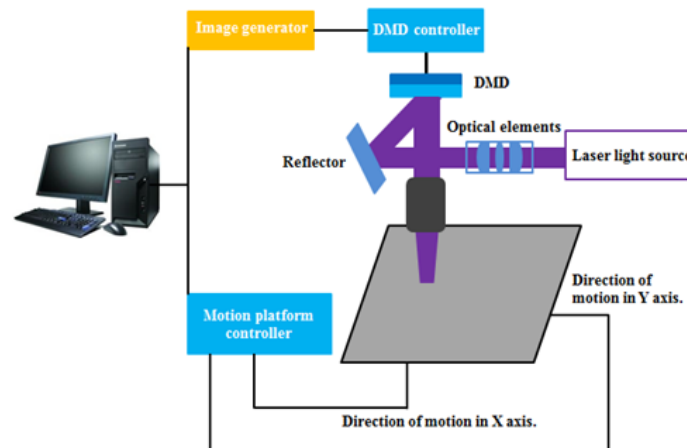


Fig. 1. DMD scanning lithography system.

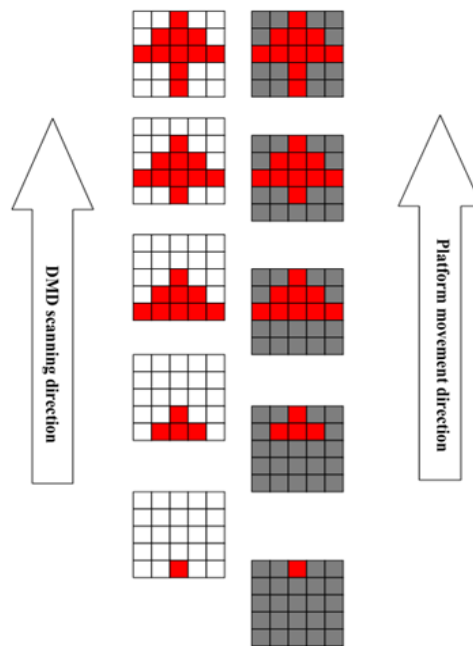


Fig. 2. Experimental principle of DMD scanning lithography.

Note that a DMD consists of numbers of micro-mirrors, and each mirror is arranged within a two-dimensional array (vertically and horizontally). Under this scenario, the input graph displayed by a DMD is two-dimensional quantized, forming a set of pattern grids. Furthermore, each micro-mirror corresponds to a quantized grid and represents one pixel. When a micro-mirror generates a rotation of  $+12$  degree, the illumination of this micro-mirror on the DMD is reflected into the projection lens and a bright pixel is formed on the photoresist substrate. When the micro mirror rotates a  $-12$  degree, the light on the same point in the DMD is not reflected into the projection lens and a dark pixel is formed on the photoresist substrate, correspondingly. Thus, the projection lens projects the graphical information created by the DMD onto the photoresist substrate, in the form of a quantized pattern with bright and dark pixels [18, 19]. In the real implementation, the moving platform is moving at a constant speed while the DMD device stands stationary. The graphic data are

introduced into the DMD line by line to realize the scrolling update of the graph displayed in the DMD. All micro-mirrors in the DMD are flipped to form a corresponding frame with each line of data inputted. The principle of scanning lithography is demonstrated in Fig. 2. For the sake of convenience, the DMD is simplified to a  $5 \times 5$  pixel array. The red grids correspond to the  $+12$  degree flip mirrors, representing bright pixels. The white grids correspond to the  $-12$  degree flip mirrors, representing dark pixels. Accordingly, a lithographic substrate is represented by a grid figure with a gray substrate. The red grids correspond to the bright area while the gray ones correspond to the dark area.

The total exposure dose of each bright area on the substrate is  $H$ :

$$H = \sum_{i=1}^m I_i \times t, \quad (1)$$

where  $I_i$  is the light intensity reflected by the micro-mirror,  $m$  is the row number of the micro-mirror array,  $t$  is the exposure time of each micro-mirror.

Moreover, the exposure time can be represented as:

$$t = \frac{L}{v}, \quad (2)$$

where  $L$  is the size of the DMD pixel,  $v$  is the speed of the moving platform.

As it is discussed in the above-stated experimental implementation, the pixel size of a DMD ( $1920 \times 1080$ ) is  $10.68 \mu\text{m}$ , and the magnification of the imaging lens is one, a minimum pixel size of the projection exposure as  $10.68 \mu\text{m}$  is obtained, consequently. As an improvement in the smoothness of the lithography pattern edge is more desirable, considerable operations are provided sequentially as is shown in the chart in Fig. 3.

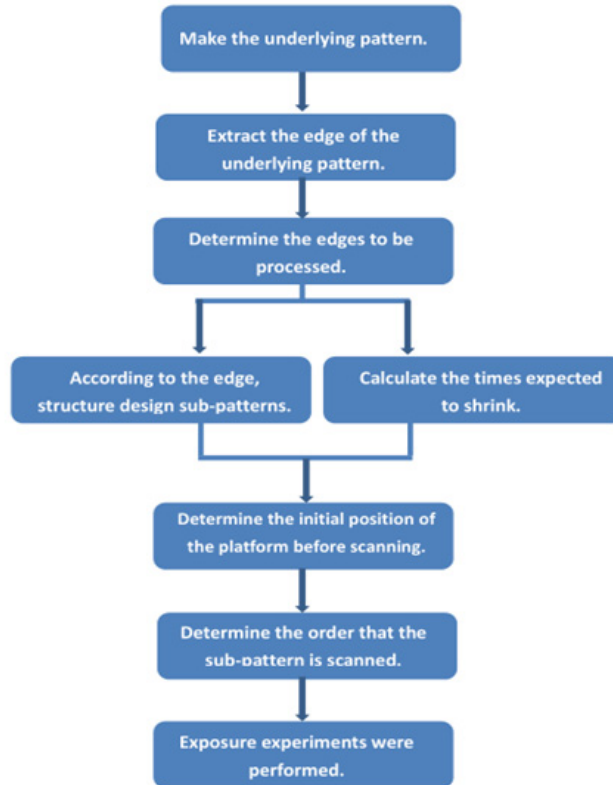


Fig. 3. Flow chart of experiment.

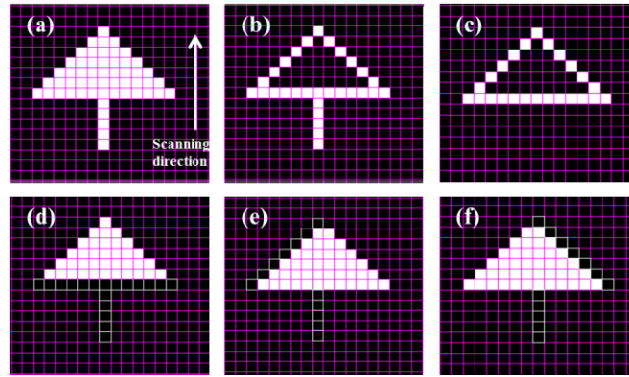


Fig. 4. The procedure of processing sub-patterns. (a) The underlying pattern, (b) Extract the edge, (c) Edges to be processed, (d) Sub-pattern 1, (e) Sub-pattern 2, (f) Sub-pattern 3.

A tree-shape lithography pattern is used to testify the method we proposed, and the process of achieving sub-patterns is described in Fig. 4. Note that each mesh picture represents a lithography pattern is introduced to the DMD (white meshes represent lithography patterns). The size of each mesh is equivalent to the size of the DMD micro-mirror (10.68  $\mu\text{m}$ ). By considering the accumulative superposition of the projection light spots from a whole column of the micro-mirrors, the lithography system automatically forms a smooth line on the lithographic substrate in the scanning direction. Thus, during the processing of the sub-patterns, the line in the scanning direction (i.e., the single white line below the white triangle in Fig. 4(a)) is ignored when only the edge of the pattern to be processed is studied, as shown in Fig. 4(c). Figures 4(d)-4(f) are sub-patterns obtained from Fig. 4(c). Figure 5 shows the procedure of stacking the sub-pattern (Fig. 4(d)) with the underlying pattern (Fig. 4(a)) to reduce the saw-tooth on both sides of the lithography pattern. The rest sub-patterns (Figs. 4(e) and 4(f)) are used to reduce the saw-tooth generated in the horizontal direction of the lithography pattern.

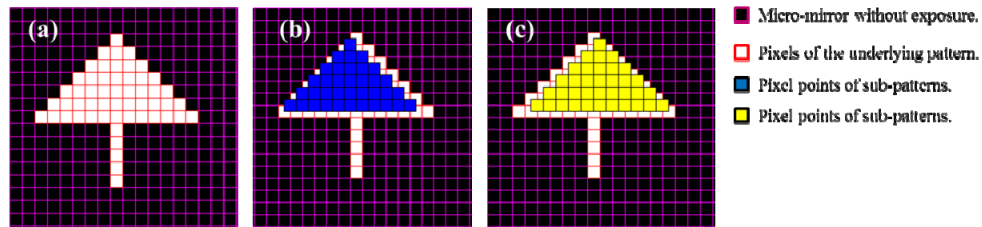


Fig. 5. Sketch map of dislocation stacking of sub-patterns. (a) No shift, (b) X: 1/2 shift (left), Y: 1/2 shift (down), (c) X: 1/2 shift (left), Y: 1/2 shift (down).

The smoothness of the lithography pattern edge is related to the DMD sub-pattern offsets (in vertical or horizontal direction) corresponding to the underlying pattern (regarded as ideally located). Note that a smaller DMD sub-pattern offset (represented as  $M_i$ ) provides a smoother edge in all lithography directions except for the scanning orientation. An equation focuses on the relation between the offset of DMD sub-patterns to the underlying pattern and the times of the saw-tooth that needed to be reduced is given in Eq. (3),

$$M_i = \frac{L}{2^i} (i = 1, 2, 3, \dots), \quad (3)$$

where  $M_i$  is the offset distance of a DMD sub-pattern relative to the underlying pattern,  $i$  is the times of the saw-tooth that needed to be reduced, and  $L$  is the size of the DMD pixel.

In the real lithography implementation, the exposure dose a substrate received should be invariable in spite of considering the ambiguity in choosing the non-wobulated DMD



scanning lithography or the wobulation technique based DMD scanning lithography. Therefore, the time ( $T$ ) required completing an exposure in the above-mentioned two lithography methods should be equivalent.

$$T = m \times t, \quad (4)$$

where  $m$  is the row number of the micro-mirror array,  $t$  is the exposure time of each micro-mirror in Eqs. (1) and (2).

Considering that multiple superimposed exposures are required in the sub-pattern lithography process, so a single exposure time can be reduced by accelerating the moving platform when the laser provides a constant intensity. According to the above discussion, the time required to achieve a single exposure of the sub-pattern ( $t'$ ) can be written as Eq. (5),

$$t' = \frac{T}{n}, \quad (5)$$

where  $n$  is the times that an exposure required to obtain the final target lithography pattern.

In order to get a high efficiency, the speed of the platform is often set at its maximum. According to Eqs. (1), (2) and (4), the time ( $T$ ) required to complete an exposure is short while the light intensity of the exposure is large. However, the moving platform cannot be accelerated infinitely. And the time required for a single exposure of the sub-pattern ( $t'$ ) is equivalent to  $T$ . So the total exposure time can be written as  $n \times T$ . In order to ensure that the exposure dose received on the lithographic substrate is the same in the multiple superimposed exposures process, the light intensity for a single exposure of the sub-pattern ( $I_w$ ) needs to be reduced. The light intensity  $I_w$  can be written as follow:

$$I_w = I_i / n. \quad (6)$$

As a result, the required total exposure time is accordingly increased in this case, in order to achieve a high-quality smoothness in lithography pattern edge.

### 3. DMD scanning lithography simulation based on a tree-shape pattern

In the lithography implementation, a portion of high spatial frequency information is filtered by the projection lens as incident light. Under this scenario, each pixel projected onto the photoresist substrate appears as a near round pixel point shares a shape close to a square. During the scanning, the toggling time of a DMD micro-mirror is consistent with the moving speed of the platform. The time the moving platform moves a distance of a micro-mirror size ( $10.68 \mu\text{m}$ ) is equal to one toggling time of a DMD micro-mirror. However, a duty cycle emerges during the exposure and the micro-mirror toggling because the mechanical inertia of the micro-mirror introduces retention. Therefore, the shape of each pixel on the photoresist substrate is stretched in the scanning direction (vertically) during the scanning exposure. In this situation, the adjacent light spots projected to the photoresist substrate form a line after the superposition of the light spots reflected by the whole column micro mirrors in the scanning direction. Consequently, the bumpy surface introduced by the DMD micro-mirror gap (approximately  $1 \mu\text{m}$  between the adjacent ones) is diminished by the exposure platform displacement. More importantly, the saw-tooth pattern on the edge of a line is automatically smoothed off in the scanning direction (i.e., the tail in the tree-shape pattern in Fig. 6). However, the resolution in the horizontal direction (vertical to the scanning orientation), restricted by the compacted size of the DMD micro-mirror, can be barely improved. In this case, only the edge of the scanning direction (represented by the tail in Fig. 6) is linearized, the other edges share a severe saw-tooth. The exposure results of lithography patterns are simulated by using MATLAB software. Figure 6 shows the simulation result of a tree-shape figure based on non-wobulated DMD scanning lithography.

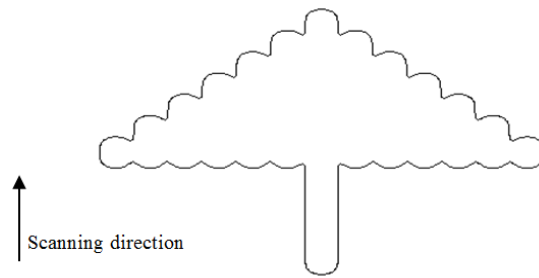


Fig. 6. Simulation result of the non-wobulation DMD scanning lithography.

In order to smooth the saw-tooth edge, an optimized sub-pattern construction method based on the wobulation technique and the DMD scanning lithography process, is proposed. Figure 7 shows the simulation results of the above-mentioned tree-shape pattern by introducing a  $1/2$  pixel sub-pattern dislocation superposition. Note that Fig. 7(a) is the scanning exposure simulation result achieved by introducing a shift corresponds to the sub-pattern (Fig. 5(b)). The shift is described as: (i) the sub-pattern shifts half a pixel to the left corresponding to the underlying pattern in the horizontal direction; and (ii) shifts half a pixel downward corresponding to the underlying pattern in the vertical direction. Figure 7(b) is another simulation result by inaugurating a shift compare to another sub-pattern (Fig. 5(c)) as well. The shift of Fig. 7(b) is: (i) the sub-pattern shifts half a pixel to the right corresponding to the underlying pattern in the horizontal direction; and (ii) half a pixel downward corresponding to the underlying pattern in the vertical direction. In addition, Fig. 7(c) is the scanning exposure pattern of Figs. 4(e) or 4(f) in the horizontal direction, relative to the underlying pattern shift half a pixel to the left or to the right (depends on the figure chosen). We want to emphasize that the smoothness difference in the horizontal edge (saw-tooth edges in Figs. 7(a) and 7(b) and the saw-tooth in Fig. 7(c)) is caused by choosing two different types of sub-patterns (one sub-pattern type as Figs. 5(a) or 5(b) and the other sub-pattern type as Figs. 4(e) or 4(f)). Finally, the combination sub-pattern shift described as a comprehensive shift among Figs. 7(a)-7(c), is introduced successively in the scanning lithography process within the underlying pattern (Fig. 5(a)). The simulation result is described in Fig. 7(d). As can be seen from Fig. 7(d), the saw-tooth in all directions except for the scanning orientation is obviously reduced.

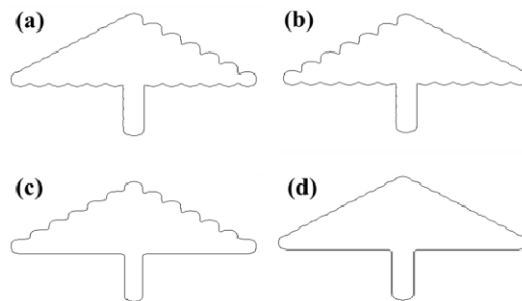


Fig. 7. Simulation results of DMD scanning lithography based on dislocation superposition principle of sub-patterns. (a) X:  $1/2$  shift (left), Y:  $1/2$  shift (down), (b) X:  $1/2$  shift (right), Y:  $1/2$  shift (down), (c) X:  $1/2$  shift (left or right), (d) the comprehensive shift.

#### 4. Evaluation of the proposed wobulation technique: Experimental results

In our experiment, a laser with a wavelength of 405 nm is chosen as the light source. A projection lens with a magnification of one is used as the projector. The SU8 photoresist used as the photosensitive material is coated on the substrate. The experimental results of non-



wobulated DMD scanning lithography observed with an optical microscope (magnification of 10) are shown in Fig. 8(a). The saw-tooth of the lithography pattern edge is deficient in all directions other than the scanning orientation (see the single line, tail-shaped pattern in Fig. 8(a)), leads to a saw-tooth size nearly 1 pixel ( $10.32\ \mu\text{m}$ ). However, in the scanning direction, the line of the edge is smooth. The lithographic patterns in a partial edge, observed by an optical microscope with a magnification of 50, are shown in Figs. 8(b) and 8(c). Note that the saw-tooth edge sizes are described as  $10.32\ \mu\text{m}$  and  $10.58\ \mu\text{m}$ , respectively. The difference in the edge sizes presented in Fig. 8(b) is caused by the stretch which is introduced by the movement in the platform scanning direction (vertical direction).

In order to reduce the saw-tooth edge effect of the lithography pattern, the exposure experiment based on the wobulation technique is carried out. We set the offset distance from the sub-pattern as half a pixel, and the cumulative times for sub-pattern as four. Note that the platform moves at a speed of  $20\ \text{mm/s}$  in the non-wobulated DMD scanning exposure. In order to guarantee the exposure dose received (the photons received by the photosensitive material on the lithographic substrate) in the wobulation technique based lithography is equivalent to that in the non-wobulated lithography, the speed of the platform is raised to  $80\ \text{mm/s}$  within a same exposure time. The experimental results are shown in Fig. 9 by introducing two optical microscopes with the magnifications of 10 (Fig. 9(a)) and 50 (Figs. 9(b) and 9(c)), respectively. As illustrated in Fig. 9(b), by introducing a  $1/2$  pixel sub-pattern dislocation superposition exposure, the size of the saw-tooth ( $5.42\ \mu\text{m}$ ) in the lithography pattern is roughly reduced by half compare to the non-wobulation lithography ( $10.32\ \mu\text{m}$ ).

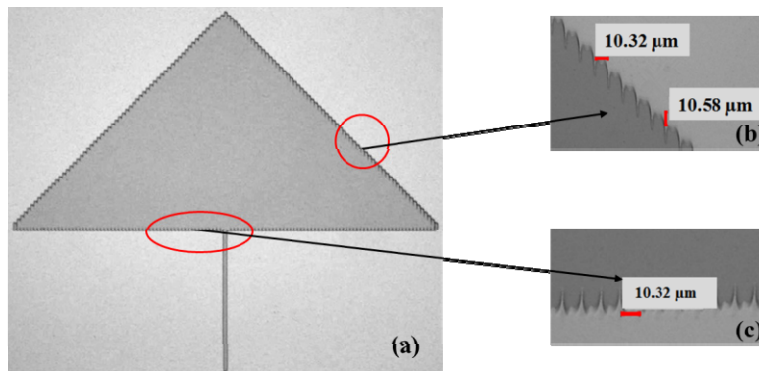


Fig. 8. Experimental results of non-wobulation DMD scanning exposure.

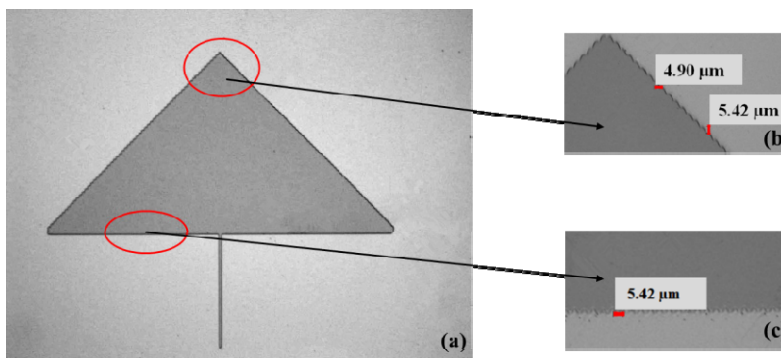


Fig. 9. Half pixel sub-pattern dislocation overlap exposure experiment.

In order to pursue a better smoothness in the edge of the lithography pattern, we conduct the lithography by reducing the distance of the sub-pattern dislocation from  $1/2$  of the original pixel to  $1/4$ , and raise the platform movement speed from  $80\ \text{mm/s}$  to  $160\ \text{mm/s}$ . The tree-

shaped lithography patterns shown in Fig. 10 are also obtained by using the two microscopes with the magnifications of 10 and 50 as mention above. Figure 10(a) presents a basically linear edge with a satisfactory smoothness. Moreover, the particular partial edge (red circle in the low right corner of Fig. 10(a)) in the lithography pattern is deeply observed with an optical microscope of magnification of 100, and the corresponding structure is shown in Fig. 11. Even though the edge structure of the lithography pattern in Fig. 11 is magnified twice compare to Fig. 10(b), the edge still proves a firmly linear edge compare to that of Fig. 10(b) with a saw-tooth size as  $0.9\ \mu\text{m}$ .

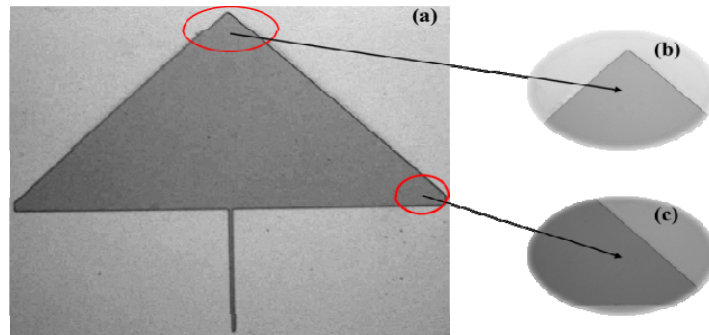


Fig. 10. 1/4 pixel sub-pattern dislocation overlap exposure experiment.

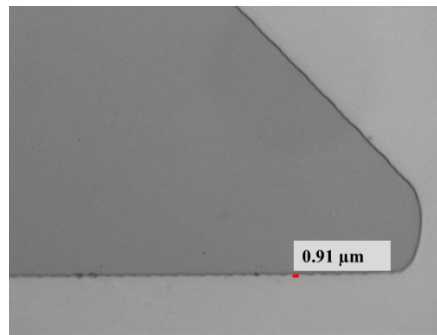


Fig. 11. Edge structure under a  $\times 100$  times microscope.

Note that the saw-tooth size should be reduced by one time when the value of the sub-pattern superposition dislocation is concentrated by half, theoretically. Namely, a 1/2 pixel sub-pattern dislocation gives a saw-tooth size as  $5.34\ \mu\text{m}$ , and a saw-tooth size as  $2.67\ \mu\text{m}$  with a 1/4 pixel sub-pattern dislocation (a saw-tooth size with a 1 pixel sub-pattern dislocation is  $10.68\ \mu\text{m}$ , the size of a DMD micro-mirror). However, the experimental results within a 1/4 pixel sub-pattern dislocation demonstrates a  $0.91\ \mu\text{m}$  saw-tooth size, representing an edge much smoother than the theoretical result. We want to emphasize that the better smoothness achieved within the 1/4 pixel sub-pattern dislocation experiment is attributed by a comprehensive effect introduced by the experimental implementation. In this case, the comprehensive effect, represented as a combination of the laser speckle effect, the projection lens distortion as well as the characterization of the moving stage, leads to a dynamic motion blur in the exposure process. In this case, the dynamic motion blur can provide a dramatic edge smoothness enhancement at a large exposure time, which will replace the sub-pattern dislocation as the first priority for the edge smoothness.

## 5. Conclusion

With the above-stated DMD scanning lithography experimental results, we proved that the edge smoothness of the lithography pattern can be significantly improved without reducing

the DMD micro-mirror size or decreasing the magnification of the projection lens by applying the wobulation technique to the DMD scanning lithography. In particular, a method to combine DMD sub-pattern dislocation superposition with continuous scanning exposure was proposed. Moreover, simulation result of the wobulation technique based DMD scanning lithography demonstrated a more favorable smoothness compare to the non-wobulation scanning lithography. The experiment implemented with a  $1/4$  sub-pattern dislocation provided a firmly linear edge within a tree-shape lithography pattern. We also demonstrated that the dynamic motion blur introduced by the experimental implementation can provide the feasibility to achieve a significant improvement in the edge smoothness. Finally, the experimental results provided that the DMD based continuous scanning exposure combined with a wobulation technique, is effective for the fabrication of high precision microstructures with large areas.

### **Funding**

Jilin Province Youth Leading Talent and Team Project (20160519021JH).

### **Acknowledgments**

This work is supported by the Innovation of Science and Technology in Jilin Province Youth Leading Talent and Team Project and s State Key Laboratory of Luminescence and Applications.